

IAC-17,A4,1,6,x38663

## MAIN RESULTS OF THE SETI-OBSERVATIONS WITH THE RATAN-600 TELESCOPE IN 2015 AND 2016 SESSIONS

A.D. Panov<sup>a\*</sup>, N.N. Bursov<sup>b</sup>, A.K. Erkenov<sup>c</sup>, L.N. Filippova<sup>d</sup>, V.V. Filippov<sup>e</sup>, L.M. Gindilis<sup>f</sup>, N.S. Kardashev<sup>g</sup>, A.A. Kudryashova<sup>h</sup>, E.S. Starikov<sup>i</sup>, J. Wilson<sup>j</sup>

<sup>a</sup> Skobeltsyn Institute of Nuclear Physics, Lomonosov Moscow state university, 1(2), Leninskie gory, GSP-1, Moscow 119991, Russian Federation, [panov@dec1.sinp.msu.ru](mailto:panov@dec1.sinp.msu.ru)

<sup>b</sup> The Special Astrophysical Observatory of the Russian Academy of Sciences (SAO RAS) Nizhnij Arkhyz, Zelenchukskiy region, Karachai-Cherkessian Republic, Russia 369167, [nmb@sao.ru](mailto:nmb@sao.ru)

<sup>c</sup> The Special Astrophysical Observatory of the Russian Academy of Sciences (SAO RAS) Nizhnij Arkhyz, Zelenchukskiy region, Karachai-Cherkessian Republic, Russia 369167, [artur@sao.ru](mailto:artur@sao.ru)

<sup>d</sup> SETI Science and Culture Center of the Tsiolkovsky Academy of Cosmonautics and by the SETI Section of the Astronomy Council, Russian Academy of Sciences. Universitetski pr., 13, Sternberg Astronomical Institute, Lomonosov Moscow State University, Moscow, Russia, [lnfilippova@yandex.ru](mailto:lnfilippova@yandex.ru)

<sup>e</sup> SETI Science and Culture Center of the Tsiolkovsky Academy of Cosmonautics and by the SETI Section of the Astronomy Council, Russian Academy of Sciences. Universitetski pr., 13, Sternberg Astronomical Institute, Lomonosov Moscow State University, Moscow, Russia, [vyfopal@gmail.com](mailto:vyfopal@gmail.com)

<sup>f</sup> Sternberg Astronomical Institute, Lomonosov Moscow State University Universitetski pr., 13, Moscow, Russia, [lmg@sai.msu.ru](mailto:lmg@sai.msu.ru)

<sup>g</sup> Levedev Physical Institute of Russian Academy of Sciences, Astro Space Center, 84/32 Profsoyuznaya st., Moscow, GSP-7, 117997, Russia, [nkardash@asc.rssi.ru](mailto:nkardash@asc.rssi.ru)

<sup>h</sup> Kazan Federal University (Department of astronomy and space geodesy), Kazan, Republic of Tatarstan, Russia, 420008, [akudryasova@yandex.ru](mailto:akudryasova@yandex.ru)

<sup>i</sup> SETI Science and Culture Center of the Tsiolkovsky Academy of Cosmonautics and by the SETI Section of the Astronomy Council, Russian Academy of Sciences. Universitetski pr., 13, Sternberg Astronomical Institute, Lomonosov Moscow State University, Moscow, Russia, [e.starikoff@gmail.com](mailto:e.starikoff@gmail.com)

<sup>j</sup> SETI@HOME project, 7481 Robinson Road Arcade, NY 14009 USA, [eagleny@gmail.com](mailto:eagleny@gmail.com)

\* Corresponding Author

### Abstract

Regular observations according to the SETI program were carried out on the Russian radio telescope RATAN-600 since 2015. The objects of observations were about 30 sun-like stars and two globular clusters with a high metallicity. The basic idea inherent the program is repeated multiple observations of the same objects. It will allow to find with guarantee a signal of duration exceeding a period of observations if it enters a transmission band of the receiver and has sufficient amplitude. Besides, this method allows to carry out a collection of a signal that allows to reveal a weak steady signal which cannot be found in a single measurement. The main results of the observations in 2015-2016 are presented in the report. The found limits of a radio emission for the objects of the used list of the SETI-candidates are given..

**Keywords:** RATAN-600, SETI, accumulation, correlation

## 1. Introduction

RATAN-600 [1] is the largest in the world (576 m aperture) radio-telescope located in Zelenchukskaya, Russia. This paper presents main results of the SETI-observations with the RATAN-600 telescope in 2015 and 2016 sessions. The RATAN-600 program of SETI observations is based on the following consideration.

One can reasonably suppose that if some cosmic civilization has a serious propensity for interstellar communication, then it can very fast in historical (or astronomical) scale of time develop many-frequency and sufficiently powerful transmitter to send interstellar messages. But if the civilization has no energy resources comparable with the power of their hosted star (in other words, it is a civilization of the first Kardashev's type) it can not transmit continuously very powerful signal to all directions simultaneously due to fundamental energetic limitations. Therefore the civilization could only scan the sky, star by star, by a strong beacon signal. Any recipient of the signal should expect only relatively short portions of the signal separated by a long periods of silence. If the civilizations of the second Kardashev's type are not a very wide-spreading phenomenon in our Galaxy, then one should not generally expect continuous messages transmitted by powerful signals from stars - SETI candidates. Therefore if somebody has observed some star - SETI candidate very carefully, with a high-sensitivity instrument, but only once during a limited period of time, and an intelligent signal from the star has not be detected, then one can not conclude that the star is not a host for a communicative civilization. This star actually may begin transmit a message exactly to the Sun system direction just at the moment when the observer begin to see in the another direction to study some other star - SETI candidate. Having no signal from a star after a single observation session of the it, one effectively has no new information about the star, supposing that our goal is to find a civilization of Kardashev's first type.

It is clear from the above that the ideal strategy of SETI search is to monitor each SETI-candidate permanently or to see continuously to all directions. Unfortunately it is technically impossible yet, supposing sufficiently high sensitivity of receivers. A reasonable compromise is to monitor a limited list of SETI candidates periodically as frequently as it is possible.

The main idea of the RATAN-600 SETI observations was to generate a limited list of SETI candidates and monitor these candidates periodically during a long period of time. This way one can restrict the maximal duration of a single message from each candidate: the maximal duration of one message can not be greater than the maximal time gap between single successive watching of the candidate. Another benefit of the program is a possibility to accumulate signal for many subsequent observations of the same object to

detect a weak signal that can not be detected in a single observation.

## 2. Methods

Observations were made at the receiver-measuring complex No.2 on the Southern sector of the RATAN-600 radio telescope with a flat reflector (Fig. 1).



Fig. 1. Receiver-measuring complex No.2 on the Southern sector of the RATAN-600 radio telescope

The observations were carried out on a three-mirror system, where the main receiving mirror is a flat reflector, and the elements of the sector of the ring antenna were installed vertically and motionless. The advantage of this mode is that it is possible to rebuild the flat reflector antenna quickly for 80-90 observations of different objects per day. The lack of such a system is, first, the loss (scattering) of energy on the surfaces of mirrors, especially on short wavelengths, and also from the misalignment of focusing, and secondly – the relatively high degree of aberration at the edges of the field of view. In such a system, there is also a relatively higher contribution from the earth's radiation, which generally leads to a loss of sensitivity relative to observations by the individual sector of the telescope by about a half, especially at high elevation angles. In the observations, the regular three-frequency complex of radiometers “Eridan-2” was used. The complex consists of three radiometers at a wavelength of 1.38, 2.7 and 6.3 cm. After a deep modernization and the abandonment of a laborious and inefficient nitrogen cooling system, the complex is represented by a warm (uncooled) set of highly sensitive radiometers with the characteristics given in Table 1.

Table 1. Characteristics of radiometers

Wavelength	1.4 cm	2.7 cm	6.3 cm
Noise temperature, K	185	100	60
Frequency band, HHZ	2.5	1.0	0.8
Expected sensitivity under 1 sec of observation, mK	5.5	5.0	3.5
Transition time	~1 sec	~2 sec	~5 sec

Radiometers for wave 2.7 and 6.3 cm worked without losses in full power mode. The sensitivity and stability of these radiometers are better than for the radiometer by a wavelength of 1.38 cm, so the data processing is done only for these wavelengths.

The observations were carried out in the wide frequency bands (see Table 1). This means that the observations were adopted to search for a powerful broadcasting beacons, but not a narrow-band signals like in the majority of other SETI programs.

### 3. Limited list of SETI objects and the statistics of the observations

The criteria to include SETI candidates to the limited SETI objects list and the candidates fulfilled these criteria were the following:

1) Sun-like stars with known planets (the number of planets shown in the brackets): HD1461 (2+2?), HD10700 (5?), HD13931 (1), HD38858 (1), HD45184 (1), HD69830 (3), HAT-P-43 (1), HD75732 (5), HD89307 (1), HD95128 (3), HD134987 (2), HD150433 (1), HD154088 (1), HD164595 (1), CoRoT-9 (1), Kepler-69 (2), Kepler-452 (1);

2) Sun-like stars close to the ecliptic plane HD50692, HD99491, HD154088, HD172051;

3) Stars-recipients of the first radio messages from the Earth: HD50692, HD75732, HD95128, HD186408, HD197076;

4) Globular star clusters NGC 6553 и PAL 10 with high metallicity (-0.18 and -0.10 respectively). Such metallicity is close to the metallicity of many stars with discovered planets, both in the environment of the Sun and at large distances. Distances to these globular clusters are 19000 ly and 20000 ly respectively.

Table 2 (see the end of the paper) shows the main properties of stars and planets— objects of the limited list. Notations in the Table 1 are the following:

- 1 - number of the star - SETI candidate in the table;
- 2 - name of the star, mainly in the Henry Draper Catalog [3];
- 3 - spectral class;
- 4 - visual star magnitude of the central star;
- 5 - distance to the star, light years;
- 6 - mass of the star, in Solar masses ( $M_{\odot}$ );
- 7 - radius of the star, in Solar radii ( $R_{\odot}$ );
- 8 - star temperature, in  $K^{\circ}$ ;
- 9 - metallicity of the star;
- 10 - star age, in billion years;
- 11 - lettered number of the planet;
- 12 - the mass of the planet in the masses of Jupiter ( $M_j$ ) is defined as  $M \sin(i)$  due to the Doppler shift in the rotation of the planetary system around the common center, where  $i$  is the slope of the plane of rotation of the planet to the line of sight (if the letter 'M' is presented near the value, then the mass estimate is determined in another way);

13 - the period of revolution of the planet around the star, in days.

The basic information on globular clusters, as well as data on stars and planets, is given by astronomical databases [4,5], databases on planetary systems and resources of the Network [6,7,8,9,10,11].

RATAN-600 telescope operated in transition mode. This means that each object may be observed only once a day during its transition through fixed antenna pattern of the telescope. Approximated transition times for various wave lengths are shown in the last row of the Table 1. Complete duration of a single record, including the time of transition near the center of the record, is typically near 2.5 min. Table 3 (see the end of the paper) lists the objects of observation, the coordinates for each object, the number of observed transitions (the number of observation days), the sum of the signal accumulation time for each object, calculated as  $t_{sum} = t_{ndays} \times t_{obs}$ , where  $t_{ndays}$  is the number of observation days;  $t_{obs}$  is the time of a single observation. The globular cluster PAL 10 was observed only ten times in 2015 and was not observed in 2016 so this object was not included in Table 3.

### 4. Results and discussion

The data of reference sources were used to process observational data for SETI objects: 0137+33 (3C48), 0237-23, 0521+16 (3C138), 0542+49 (3C147), 0627-05 (3C161), 1154-35, 1256-05, 1331+30 (3C286), 1347+12, 1411+52 (3C295), 1459+71 (3C309.1), 1850-01, 2107+42 (NGC7027), covering all visible sky. Based on the processed data from the reference sources, the curves of the conversion of the antenna temperatures into the flux density at wavelengths of 2.7 and 6.2 cm were constructed.

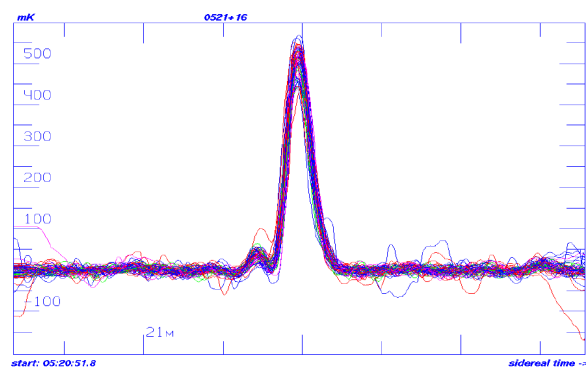


Fig. 2. Sixty five overlapped records (observations of transitions through the RATAN-600 antenna pattern) on wavelength 2.7 cm of the reference source 0521+16 (quasar 3C138 with coordinates RA: 05:21:9.89, Dec: 16:38:22.10 (J2000)). The division on the time scale is 5 seconds.

A plot with 65 overlapped records of the reference point-like source 0542+49 (3C147) on the wavelength 2.7 cm are shown in Fig. 2. The shape of the line reproduces the shape of the antenna pattern of RATAN-600 telescope. The side lobe of the antenna pattern is seen to the left of the main peak. It is generally expected that a source of an artificial signal will demonstrate similar shape of peak in the records of objects – SETI-candidates. If the signal would sufficiently strong it can be observed in a single (one-transition) record above the background noise around the peak. No such strong signals, having the expected point-like shape of the transition peak (Fig. 2), were found in the directions of SETI-candidates.

If a signal actually exists but it is too low to be discovered in a single observation, then it still may be discovered after accumulation of the peak through many records. The accumulation method was implemented in preprocessing of the data.

When searching for weak signals by the accumulation method, all the entries of SETI objects after a necessary preliminary processing were divided into two independent equal groups  $Sum_1$  and  $Sum_2$ , according to their variances. In each group, the Hodges-Lehmann method was used to find the averaged signal and the following combinations were calculated:

$$Sum = (Sum_1 + Sum_2) / 2$$

$$Dif = (Sum_1 - Sum_2) / 2$$

If the measurements were carried out correctly and the possible signal was independent of time, then  $Sum$  must be the sum of the noise and the signal, and the value of  $Dif$  must be a pure noise. This assumption was tested to verify the correctness of the measurement procedure and to search for possible anomalies in it.

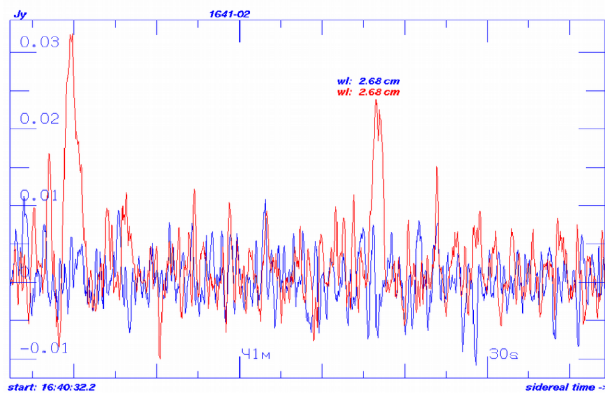


Fig. 3.  $Sum$  (red) and  $Dif$  (blue) signals for HD 150433 (1641-02) candidate.

$Sum$  and  $Dif$  signals for two years of accumulation (182 records) for HD 150433 candidate are shown in Fig. 3. It is seen that the  $Dif$  signal actually has no deviation from pure noise behavior. But the  $Sum$  signal shows signs of two statistically significant peaks.

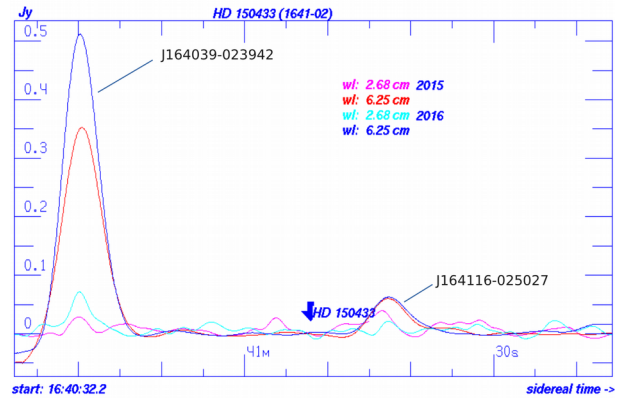


Fig. 4. Results of accumulation of the signal for the HD 150433 (1641-02) candidate separately for 2015 and 2016 years and separately for two different wavelengths 2.7 cm and 6.3 cm

Fig. 4 shows the results of accumulation of the signal for the same HD 150433 (1641-02) candidate separately for two years of observations 2015 and 2016 and separately for two different wavelengths 2.7 cm and 6.3 cm. The signals are smoothed with antenna pattern width in Fig. 4. The expected position of HD 150433 signal is pointed out by a blue arrow. Two statistically significant signals of Fig. 3 are seen also in Fig.4 and correspond actually for two known radio sources J164039-023942 (350-500 mJy) and J164116-025027 (~50 mJy) from the NVSS catalog [12,13]. However there is no sign of a signal in the place of the expected position of HD 150433 source.

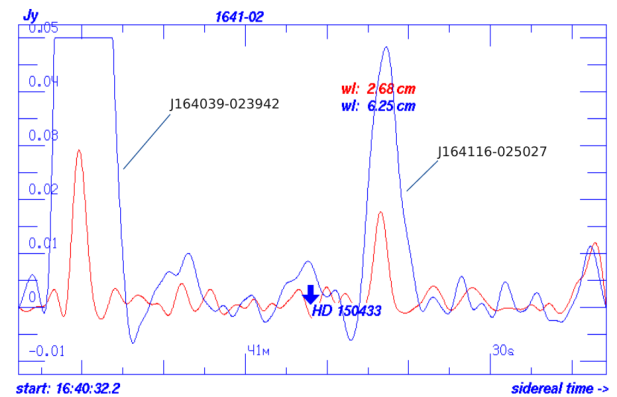


Fig. 5. Results of accumulation of the signal for the HD 150433 (1641-02) candidate with all the statistics in 2015 and 2016; separately for two different wavelengths 2.7 cm and 6.3 cm.

The signals for the HD 150433 (1641-02) candidate accumulated for all the statistics in 2015 and 2016; separately for two different wavelengths are shown in

Fig. 5. This picture confirm that there is no statistically significant signal from the direction of this candidate.

Similar analysis was repeated for each candidate. Known level of noises permitted us to estimate upper bound for the signals of all candidates. Table 4 shows these data at three-sigma level for all candidates of the limited list. No signs of statistically significant fluxes from them were found.

Another method of searching for broadband signals for SETI candidates was to search for the correlation of signals at two wavelengths of 2.7 cm and 6.3 cm. To obtain the coefficients of linear correlation, the data sets for each source were matched according to the observation time. The difference between the number of observation days on different waves was due primarily to external noises that can occur independently in different frequency bands, and also sometimes by non-working radiometers on a particular wave.

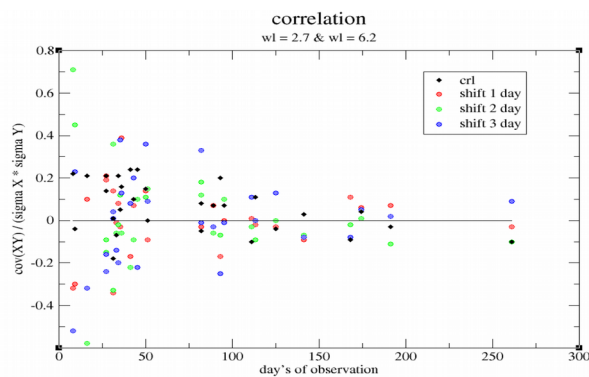


Fig. 6. Linear correlation between the data at 2.7 and 6.3 cm wavelengths (black diamonds). Test shifts of 1,2,3 days - colored circles.

Linear correlation between the data at 2.7 and 6.3 cm wavelengths for all candidate sources is shown in Fig. 6. There are also variants of shifting one time series relative to another by 1, 2 and 3 days, in order to evaluate the nonrandomness of the correlation obtained. The average value of the correlation coefficient is  $r_{avr} = 0.06 \pm 0.12$ , and it does not depend on the shifts of the arrays. This indicates that there is no correlation between the wavelengths. This is especially evident with large data sets. Therefore, correlation analysis also show no signs of real signals from the SETI candidates of the limited list.

## 5. Conclusion

In the SETI-sessions on the RATAN-600 radio telescope in 2015 and 2016, signs of artificial origin signals were not found. However, data analysis showed that observations on a large radio telescope, which is RATAN-600, allow to accumulate a signal from SETI objects with high sensitivity - up to 1 mJy, and to

monitor their radiation with a flux stability of several percent of the received signal level. Work on the SETI program on the RATAN-600 telescope continues.

## References

- [1] Handbook of RATAN-600 Continuum observer, ver.0.3 (Oct 1998), [https://www.sao.ru/hq/iran/ratan/ratan\\_english.html](https://www.sao.ru/hq/iran/ratan/ratan_english.html) (accessed 04.09.17)
- [2] Filippova L.N. and Strel'nitskij V.S. Ecliptic as an "Attractor" for SETI. *Astron. Tsirk.*, 1531 (1988) 31 – 32.
- [3] ARI Data Base for Nearby Stars. ARICNS stars in the Henry Draper Catalogue (HD) or in the HD Extension (HDE). <http://wwwadd.zah.uni-heidelberg.de/datenbanken/aricns/hd.htm> (accessed 04.09.17)
- [4]. SIMBAD Astronomical Database, <http://simbad.u-strasbg.fr/simbad/> (accessed 04.09.17).
- [5]. The VizieR Service for Astronomical Catalogues (CDS, Strasbourg, France), <http://vizier.u-strasbg.fr/> (accessed 04.09.17).
- [6]. NASA exoplanet archive, <https://exoplanetarchive.ipac.caltech.edu/index.html> (accessed 04.09.17).
- [7]. The Exoplanet Data Explorer, <http://exoplanets.org/table> (accessed 04.09.17).
- [8]. Exoplanet.eu, <http://exoplanet.eu/catalog/> (accessed 04.09.17).
- [9]. Planetary systems (in Russian), <http://www.allplanets.ru/index.htm> (accessed 04.09.17).
- [10]. Genya Takeda, Eric B. Ford, Alison Sills, Frederic A. Rasio, Debra A. Fischer, and Jeff A. Valenti. Structure and Evolution of Nearby Stars with Planets II, [http://exoplanets.astro.yale.edu/science/analysis/spocs\\_evol.php](http://exoplanets.astro.yale.edu/science/analysis/spocs_evol.php) (accessed 04.09.17).
- [11]. William E. Harris. Catalog of parameters for Milky Way globular clusters: the database, <http://physwww.physics.mcmaster.ca/~harris/mwgc.dat> (accessed 04.09.17).
- [12] J.J. Condon, W.D. Cotton, E.W. Greisen, Q.F. Yin, R.A. Perley, G.B. Taylor, J.J. Broderick. The NRAO VLA Sky Survey. *Astronomical Journal*, 115 (1998) 1693.
- [13] J.J. Condon, W.D. Cotton, E.W. Greisen, Q.F. Yin, R.A. Perley, G.B. Taylor, J.J. Broderick. The NRAO VLA Sky Survey. <http://www.cv.nrao.edu/nvss/> (accessed 04.09.17)

Table 2. Properties of stars and planets– objects of RATAN-600 observations

№	Name star	Spctr type	V_mag [ m ]	Dist [ly]	M [M <sub>☉</sub> ]	R [R <sub>☉</sub> ]	T [K]	Fe/H	Age [Gyr]	Planet	M [M <sub>J</sub> ]	P [day]
(1)	(2)	(3)	(4)	(5)	(6)	(7)	(8)	(9)	(10)	(11)	(12)	(13)
1	HD 1388	G0V	6.51	84.8	1.05	1.13	5952	-0.04	4.88	?	?	
2	HD 1461	G0V	6.5	76		1.02	5765		4.2-7.1	b	6.9	5.77
										c	5.9	13.5
3	HD 13931	G0	7.2R	14	1.04		5868	0.03	8.4	b	1.88	4218
4	HD 38858	G4V	5.97	49.5	0.89	0.93	5723	0.24	6.2	b	0.09	407
5	CoRoT-5	F9V	14	1304	1.00	1.19	6100	0.25	5.5-8.3	b	0.46	4.04
6	HD 50692	G0V	5.74	56	1.1	1.03	6024		5.5	?		
7	HD 51419	G5V	6.94	80.3	1.0	-	-	-	-	-	0.168	1096
8	HD 69830	G8V	5.98	40.7	0.86	0.91	5394	0.04	10.6	b	10.2	8.67
										c	11.8	31.6
										d	18.1	197
9	HAT-P-43		13.4	1771	1.05	1.10	6000	0.23	5.7	b	0.66	3.33
10	HD 75732A	G8V	5.95	40.9	0.95	0.94	5196	0.31	10.2	b	0.824	14.65
										c	0.169	44.34
										d	3.835	5218
										e	0.025	0.737
										f	0.144	260.7
11	HD 89307	G0V	7.06	108	1.03	1.05	5950	0.14	6.76	b	2	2199
12	HD 95128	G0-1V	5.03	45.9	1.08	1.17	5887	0	7.4	b	2.53	1078
										c	0.54	2391
										d	1.64	10000
13	83 Leo B	K2V	?	57.61	0.88	0.81	?	?	?	b	0.11	17.04
14	HD 114783	K0V	7.57	66.60	0.92	0.78	5105	0.33	3.7	b	1.1	493.7
15	HD 134987	G5V	6.45	72.41	1.07	1.25	5740	0.25	9.7	b	1.59	258.2
										c	0.82	5000
16	HD 146233	G2V	5.56	15.90	1.01	1.02	5800	0.05	4.2	?		
17	HD 150433	G0	7.22	29.6	1.0	?	?	?	?	b	0.168	1096
18	HD 154088	K0IV	6.58	17.8	0.9	?	?	?	?	b	0.0193	18.6
19	HD 157347	G3V	6.28	63	0.98	1.02			6.64			
20	HD 164595	G2V	7.1	94.36	0.99	?	5790	0.04	?	b	0.052	40
21	HD 164922	G9V	6.99	72.18	0.87	1.00	5293	0.16	13.4	b	0.34	1201

No	Name star	Spctr type	V_mag [ m ]	Dist [ly]	M [M $\odot$ ]	R [R $\odot$ ]	T [K]	Fe/H	Age [Gyr]	Planet	M [Mj]	P [day]
										c	0.041	75.76
22	HD 172051	G6V	5.86	42.3	0.93	0.86	5580	0.21	?			
23	CoRoT-25	G0V	15.0	3261	1.09	1.19	6040	0.01	5.2	b	0.27M	4.86
24	CoRoT-9	G3V	13.7	1500	0.99	0.94	5625	0.01	4	b	0.84M	95.27
25	Kepler-6	?	13.3B	-	1.21	1.39	5647	0.34	3.8	b	0.67M	3.234
26	HD186408 A HD186408 B	G1.5 V	5.96 6.20	66.8	1.02 0.97	1.7 1.2	5803 5752	1.14 1.23	10.4 9.9	?		
27	HD 197076	G5V	6.44	?	1.00	1.00	-	-	3.80	?		
28	HD 217877	G0-V	6.68	100.4	?	-	-	-	-	?		

Table 3. List of SETI-objects and their observation time at RATAN-600 in 2015-2016.

n	source name	R.A (2000) [hh:mm:ss]	Dec (2000) [dd:mm:ss]	days of observation	time (min) of observation	observation short name
1	HD 1388	00:17:58.87	-13:27:20.3	52	125	0017-13
2	HD 1461	00:18:41.86	-08:03:10.8	77	185	0018-08
3	HD 13931	02:16:47.37	+43:46:22.7	31	74	0216+43
4	HD 38858	05:48:34.94	-04:05:40.7	54	130	0548-04
5	CoRoT-5	06:45:06.54	+00:48:54.8	108	259	0645+00
6	HD 50692	06:55:18.66	+25:22:32.5	9	22	0655+25
7	HD 51419	06:58:11.75	+22:28:33.2	17	41	0658+22
8	HD 69830	08:18:23.94	-12:37:55.8	27	65	0818-12
9	HAT-P-43	08:35:42.17	+10:12:23.9	27	65	0835+10
10	HD 75732	08:52:35.81	+28:19:50.9	34	82	0852+28
11	HD 89307	10:18:21.28	+12:37:15.9	82	197	1018+12
12	HD 95128	10:59:27.97	+40:25:48.9	41	98	1059+40
13	83 Leo B	11:26:45.28	+03:00:22.18	8	19	1126+03
14	HD 114783	13:12:43.78	-02:15:54.1	45	108	1312-02
15	HD 134987	15:13:28.66	-25:18:33.6	53	127	1513-25
16	HD 146233	16:15:37.26	-08:22:09.0	186	446	1615-08
17	HD 150433	16:41:08.21	-02:51:26.2	182	437	1641-02
18	HD 154088	17:04:27.84	-28:34:57.6	123	295	1704-28
19	HD 157347	17:22:51.28	-02:23:17.4	192	461	1722-02
20	HD 164595	18:00:38.89	+29:34:18.9	210	504	1800+29
21	HD 164922	18:02:30.86	+26:18:46.8	37	89	1802+26
22	NGC 6553	18:09:15.68	-25:54:27.9	35	84	1809-25

n	source name	R.A (2000) [hh:mm:ss]	Dec (2000) [dd:mm:ss]	days of observation	time (min) of observation	observation short name
23	HD 172051	18:38:53.40	-21:03:06.7	99	238	1838-21
24	CoRoT-25	18:42:31.11	+06:30:49.7	130	312	1842+06
25	CoRoT-9	18:43:08.81	+06:12:14.8	146	350	1843+06
26	Kepler-69	19:33:02.62	+44:52:08.0	106	254	1933+44
27	HD 186408	19:41:48.95	+50:31:30.2	101	241	1941+50
28	HD 197076	20:40:45.14	+19:56:07.9	276	662	2040+19
29	HD 217877	23:03:57.27	-04:47:41.4	54	130	2303-04

Table 4. List of SETI-objects and estimations of flux density (mJy)

n	source name	2015 2.7 cm	2015 6.3 cm	2016 2.7 cm	2016 6.3 cm	observation short name
1	HD 1388	< 7	< 9	< 6	< 5	0017-13
2	HD 1461	< 61	< 7	< 108	< 4	0018-08
3	HD 13931	< 9	< 25	< 14	< 18	0216+43
4	HD 38858	< 41	< 6	< 28	< 8	0548-04
5	CoRoT-5	< 8	< 9	< 6	< 17	0645+00
6	HD 50692	< 8	< 17	< 9	< 8	0655+25
7	HD 51419	< 12	< 22	< 7	< 7	0658+22
8	HD 69830	< 13	< 7	< 6	< 4	0818-12
9	HAT-P-43	< 6	< 12	< 8	< 4	0835+10
10	HD 75732	< 8	< 15	< 12	< 12	0852+28
11	HD 89307	< 5	< 4	< 5	< 5	1018+12
12	HD 95128	< 11	< 15	< 11	< 23	1059+40
13	83 Leo B	< 8	< 19	< 14	< 10	1126+03
14	HD 114783	< 9	< 7	< 5	< 7	1312-02
15	HD 134987	< 8	< 7	< 5	< 11	1513-25
16	HD 146233	< 27	< 6	< 65	< 8	1615-08
17	HD 150433	< 12	< 13	< 6	< 8	1641-02
18	HD 154088	< 17	< 8	< 6	< 5	1704-28
19	HD 157347	< 9	< 4	< 5	< 5	1722-02
20	HD 164595	< 2	< 5	< 3	< 4	1800+29
21	HD 164922	< 28	< 12	< 10	< 14	1802+26
22	NGC 6553	< 15	< 14	< 9	< 18	1809-25
23	HD 172051	< 7	< 7	< 6	< 9	1838-21
24	CoRoT-25	< 3	< 5	< 2	< 4	1842+06
25	CoRoT-9	< 4	< 3	< 4	< 5	1843+06

n	source name	2015 2.7 cm	2015 6.3 cm	2016 2.7 cm	2016 6.3 cm	observation short name
26	Kepler-69	< 9	< 9	< 7	< 21	1933+44
27	HD 186408	< 12	< 13	< 11	< 28	1941+50
28	HD 197076	< 2	< 5	< 3	< 4	2040+19
29	HD 217877	< 61	< 16	< 35	<9	2303-04